GHENT
UNIVERSITY

This is the peer-reviewed author-version of:

An IR Spectroscopy Study of the Degradation of Surface Bound Azido-Groups in High Vacuum

Reference

Vandenbroucke, Sofie ST, Mikko Nisula, Robin Petit, Rita Vos, Karolien Jans, Philippe M. Vereecken, Jolien Dendooven, and Christophe Detavernier. "An IR Spectroscopy Study of the Degradation of Surface Bound Azido-Groups in High Vacuum." *Langmuir* 37, no. 43 (2021): 12608-12615.

Full text (Publisher's DOI): https://doi.org/10.1021/acs.langmuir.1c01903

An IR spectroscopy study of the degradation of surface bound azido-groups in high vacuum

Sofie S. T. Vandenbroucke,[†,‡] Mikko Nisula,[†] Robin Petit,[†] Rita Vos,[‡] Karolien Jans,[‡] Philippe M. Vereecken,[¶,‡] Jolien Dendooven,[†] and Christophe Detavernier[*,†]

[†]*Department of Solid State Sciences, CoCooN group, Ghent University, Krijgslaan 281 (S1), 9000 Gent, Belgium*

[‡]*Interuniversity Micro Electronics Center (IMEC), Kapeldreef 75, B-3001 Leuven, Belgium*

[¶]*Centre for Surface Chemistry and Catalysis, KU Leuven, Celestijnenlaan 200F, B-3001 Leuven, Belgium*

E-mail: christophe.detavernier@ugent.be

Abstract

Controlled surface functionalization with azides to perform on surface 'click chemistry' is desired for a large range of fields such as material engineering and biosensors. In this work, the stability of an azido-containing self-assembled monolayer in high vacuum is investigated using in situ Fourier transform infrared spectroscopy. The intensity of the antisymmetric azide stretching vibration is found to decrease over time, suggesting the degradation of the azido-group in high vacuum. The degradation is further investigated at three different temperatures and at seven different nitrogen pressures ranging from 1×10^{-6} mbar to 5×10^{-3} mbar. The degradation is found to increase at higher temperatures and at lower nitrogen pressures. The latter supporting the theory that the degradation reaction involves the decomposition into molecular nitrogen. For the condition with the highest degradation detected, only 63 % of azides is found to remain

at the surface after 8 h in vacuum. The findings show a significant loss in control of the surface functionalization. The instability of azides in high vacuum should therefore always be considered when depositing or post-processing azido-containing layers.

Keywords

Azide, vacuum, stability, FTIR, self-assembled monolayer, surface functionalization

1 Introduction

'Click chemistry' is an approach defined by Sharpless and coworkers in 2001,[1] as a foundation to join small building blocks together to various complex compounds, based on nature's way of synthesising natural products. The term encompasses a set of powerful chemical reactions that: (i) use readily available starting materials, (ii) proceed under benign conditions, (iii) have high yield, (iv) are stereospecific, (v) are orthogonal to other reactions, (vi) generate inoffensive by-products and (vii) produce stable products.[1,2] The desired characteristics of click reactions open up synthesis pathways in various application fields[2–4] such as drug discovery,[5,6] polymer chemistry,[7,8] materials engineering,[9,10] bioconjugation[11–13] and biosensors.[14–17] The azide-alkyne Huisgen 1,3-dipolar cycloaddition yielding 1,2,3-triazoles, via a copper-catalysed or strain promoted reaction, is considered the cream of the crop of the click reactions.[1,18–20] Azido-moities are not only highly useful for click reactions. One can easily transform the azide moities into other useful functional moieties such as amines or thiocyanates via a nucleophilic substitution using a halide atom.[21,22]

Surface functionalization with azido-containing self-assembled monolayers (N_3-SAMs) can be achieved by for example using organosilanes. This typically involves solution-phase protocols starting from the introduction of azido-containing moieties to the surface via spin-coating or liquid-phase silanization, to the performance of the click reaction itself.[23–29] How-

ever, vapour-phase chemistry is beneficial regarding integration into a high-throughput production sequence, yielding high-quality and reproducible results with a reduced chemical waste production. The deposition of N_3-SAMs from the vapour-phase has been demonstrated[30,31] as well as the use of the on-surface azide-alkyne click reaction from the vapour-phase to deposit 2D nanostructures.[32,33] Moreover, azide and alkyne based precursors have been used to grow thin bis-triazole organic films via atomic and molecular layer deposition (ALD/MLD).[34,35]

Vapour-phase chemistry often requires the use of (ultra) high vacuum techniques. For the development of novel vapour phase fabrication methods, the stability of the azido group in high vacuum conditions is of utmost importance. In addition, since several processing steps in semiconductor industry utilize high vacuum techniques, the azido-groups need to be stable during all post-functionalization steps in the production process. The stability of azides upon X-ray exposure,[36,37] irradiation by UV-light[38–41] and heating[41–44] has extensively been studied in the past. To our knowledge, only a few literature reports mention the degradation of azido-groups in high vacuum such as the work of Bebensee et al.,[33] Diaz et al.[32] and Gao et al.[45] However, no detailed study of the stability of azides in high vacuum has previously been performed. In this work, the degradation of azides in high vacuum is monitored using in situ reflection Fourier transform infrared spectroscopy. This technique allows to observe real-time changes in IR absorbance of the functional groups at the surface while in high vacuum. In addition, the used IR light will not result in the decomposition of the azides, in contrast to UV- or X-ray-based techniques. The degradation of the azido-groups in high vacuum is further studied for different temperatures and nitrogen pressures, as it is believed that the degradation reaction involves the decomposition into molecular nitrogen.

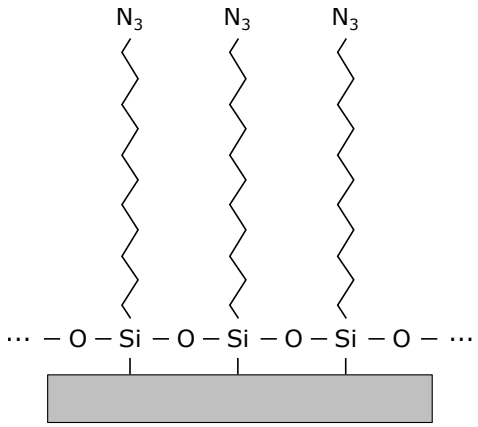

Figure 1: Schematic illustration of a N_3-SAM coated oxide surface.

2 Experimental

Azido-containing self-assembled monolayers (N_3-SAM) are deposited by vapour phase silanization. All substrates are cleaned prior to deposition using UV ozone (UVO cleaner, Jelight Company Inc.). The silanization is performed using a home-built stainless-steel vacuum chamber at a pressure of 25 mbar, heated inside a WU 6100 Thermo Scientific oven at 145 °C. During a deposition time of 2 h, 120 µL 11-azidoundecyltrimethoxysilane (abcr GmbH.) is evaporated inside the chamber. The process is described in more detail by Vos et al.[31] A schematic illustration of the coated surface is given in Figure 1.

Characterization of SAMs is often performed using contact angle measurements, spectroscopic ellipsometry, X-ray photoelectron spectroscopy (XPS), atomic force microscopy or Fourier transform infrared spectroscopy (FTIR).[24,25,46,47] In the current work, FTIR is chosen as the main experimental technique to study chemical changes at the surface by the degradation of the N_3-SAM in high vacuum. Azides can easily be identified using FTIR due to their strong IR absorbance outside the fingerprint region. In addition, the technique provides chemical information without the need of a high vacuum chamber to perform the measurement or the use of an irradiation source that might cause photo-oxidation of the azido-groups such as an UV- or X-ray irradiation. Furthermore, the degradation during

the high vacuum treatment can be studied using in situ FTIR, which has previously been demonstrated to be a very sensitive technique to measure changes of chemical bonds at the surface.[48]

Silicon samples coated with 70 nm TiN and a 3 nm thin film of SiO_2 are used as the substrate for the N_3-SAM deposition, to facilitate in situ reflection FTIR experiments. The TiN layer is deposited by reactive sputtering using nitrogen gas and a Ti target (Endura, Applied Materials Inc.). The SiO_2 is RF-sputtered in argon gas using a SiO_2 target (Leybold AG, 99.995%). The degradation of the N_3-SAM is monitored by in situ FTIR spectroscopy inside a home-built vacuum chamber with a base pressure of 1×10^{-5} mbar. The vacuum chamber is attached to a Vertex 70V spectrometer (Bruker Co.) via KBr windows. The grazing incident mid-IR beam is aligned on the sample surface with an angle of ca. 83° with respect to the normal plane of the sample surface via off-axis parabolic mirrors in order to enhance the sensitivity.[49–51] The reflected IR signal is detected with a resolution of $4\,\mathrm{cm}^{-1}$ using a medium band mercury cadmium telluride (MCT) detector cooled with liquid nitrogen. Each spectrum is generated by averaging over ~ 206 scans, corresponding to a measurement time of 2 min.

A background spectrum is recorded after pumping the chamber to base pressure and heating the sample to 150 °C with a PID-controlled copper heating stage. From this moment, FTIR spectra are recorded every 7 min for approximately 8 h. This allows us to observe all functional groups changing over time in vacuum compared to the initial spectrum of the as-deposited sample. Data analysis is performed with Python.[52] The background during the experiment evolves, mainly due to thermal changes inside the detector and vacuum chamber. This background evolution is approximated and subtracted to obtain the final spectra used for peak analysis in this work. An illustration of the calculated background and final spectrum can be found in the supporting information Figure S1 together with a brief description of the Python procedure.

Silicon samples with a native oxide are used as substrate for the N_3-SAM depositions to analyse the influence of the sample temperature and N_2-pressure on the N_3 degradation using ex situ attenuated total reflection FTIR (ATR-FTIR). For this purpose, a different setup is used than the in situ FTIR vacuum chamber described earlier, a home-built vacuum chamber with a base pressure of 1×10^{-6} mbar. Herein, the samples are exposed to a pre-set temperature and N_2-pressure for 8 h while pumping. The sample temperature is PID-controlled using a copper heating stage and set to 90 °C, 120 °C or 150 °C. The lowest temperature is defined by the minimum sample temperature that can be obtained, while heating the chamber walls to 100 °C to prevent the condensation of water. The highest temperature is chosen to be close to the silanization temperature of 145 °C and well below the thermal decomposition temperature of 180 °C reported for alkyl azides in literature.[42,43] The N_2-pressure (Air Liquide S.A., 99.999%) inside the chamber is read-out with a compact full range pressure gauge PKR 251 (Pfeiffer Vacuum GmbH) and adjusted to values between 1×10^{-6} mbar to 5×10^{-3} mbar using a needle valve. The lower limit is defined by the chamber's base pressure, while the upper limit is set to 5×10^{-3} mbar in order to remain below the maximum operating pressure of the turbomolecular pumping system.

Ex situ ATR-FTIR is performed with a Nicolet 6700 spectrometer using a liquid-nitrogen cooled MCT detector (Thermo Fischer Scientific Inc.) and a VariGATR grazing angle accessory with a Ge-crystal (Harrick Scientific Products Inc.). An ATR-FTIR spectrum with a spectral resolution of 4 cm^{-1} is generated by averaging over 100 scans. The N_3-peak area is calculated with a fixed integration method in OPUS (Bruker Co.). The samples are compared to an untreated N_3-SAM and blank Si reference to calculate the percentage of azide remaining.

Ex situ transmission FTIR measurements are performed with the same Vertex 70V spectrometer (Bruker Co.) using a different beam path and a DLaTGS detector. The spectrometer is pumped to vacuum (approximately 1×10^{-2} mbar) for 15 min in between measurements in

order to obtain constant background levels of atmospheric gases. The IR-signal is detected for a measurement time of 3 min ($\sim$ 214 scans) and a resolution of 4 cm^{-1}. A blank Si reference is subtracted from the raw data to be able to observe all chemical bonds originating from the N_3-SAM coating.

Contact angle measurements are performed with a DSA 30 contact angle system (Krüss GmbH) in sessile drop mode with drops of 1 µL. Analysis is done using the tangent I method. The contact angles reported in this work are the average of five contact angle measurements taken on different positions of the sample.

3 Results and Discussion

The functional groups of the as-deposited N_3-SAM samples as observed by transmission FTIR can be seen in Figure 2 a. Background noise is observed in the regions 4000 cm^{-1} to 3400 cm^{-1}, 1700 cm^{-1} to 1400 cm^{-1} and around 2330 cm^{-1}, originating from residual atmospheric water vapour and CO_2 inside the spectrometer. In addition, features due to organic contamination from air exposure are visible with the most prevalent band observed at 1723 cm^{-1}, typically assigned to C=O.[31,53,54] In the region from 3000 cm^{-1} to 2800 cm^{-1} clear bands of CH_3 and CH_2 stretching vibrations are observed. Inevitably these are partially the result of organic contamination at the surface. However, the high intensity of the CH_2 stretching vibrations confirms the presence of the alkane chain with 11-carbon atoms onto the surface. The antisymmetric and symmetric CH_2 stretching vibrations are occurring at 2925 cm^{-1} and 2855 cm^{-1} respectively, while the CH_2 scissor mode is seen at 1450 cm^{-1}.[55–57] The unexpected strong intensity of the CH_2 scissor mode compared to the CH_2 streching vibrations can be explained by the background subtraction as shown in Figure S2 in supporting information. The azido-group N_3 is characterized by its antisymmetric stretching band at 2098 cm^{-1}. It is less obvious to distinguish the symmetric stretching band of N_3 between 1345 cm^{-1} to 1175 cm^{-1} as it is weak in intensity and overlaps with the CH_2 bending

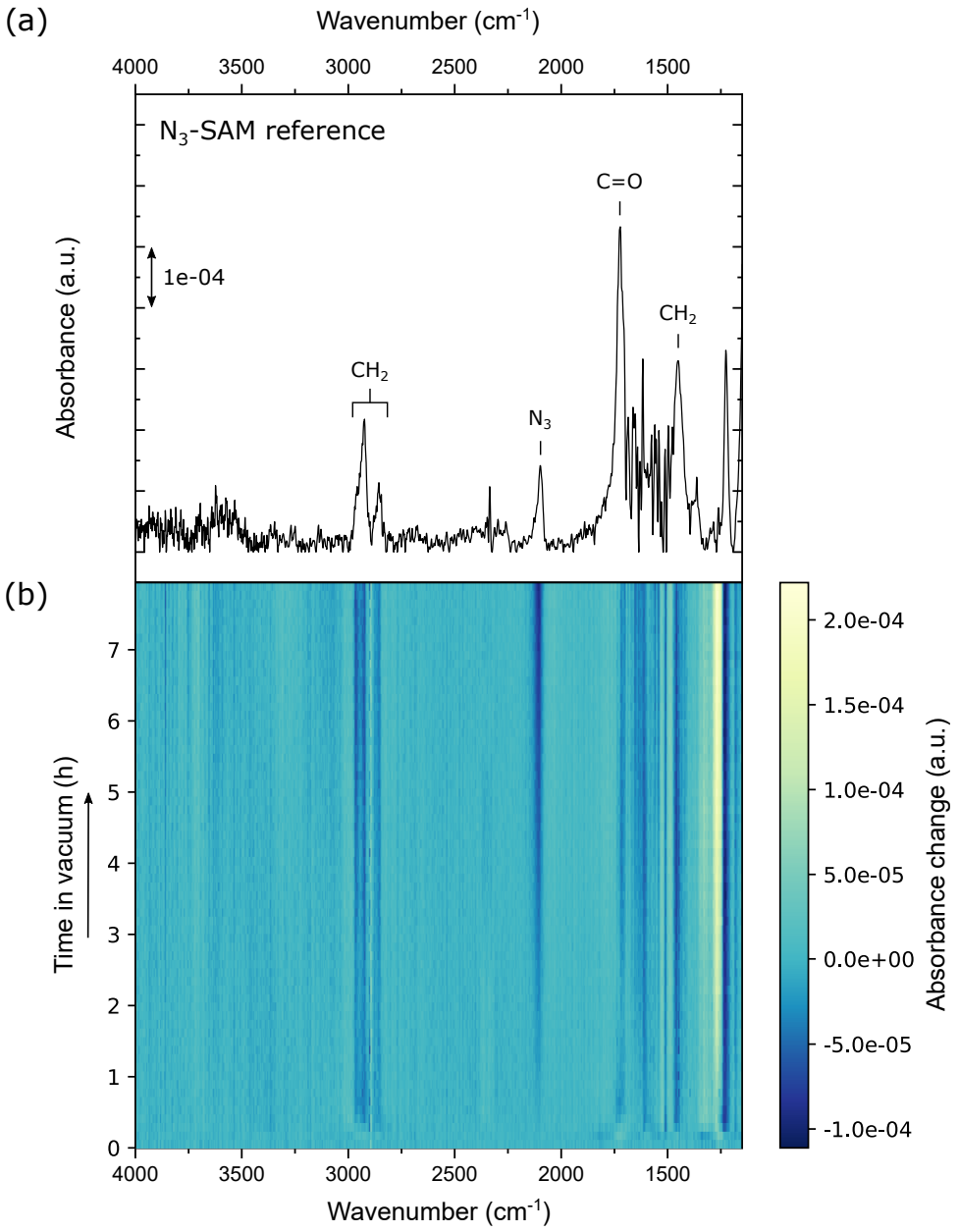

Figure 2: An ex situ transmission FTIR spectrum indicating the functional groups of the as-deposited N_3-SAM (a) and the time evolution of the change in IR absorption intensity in high vacuum at 1×10^{-5} mbar and 150 °C over 8 h as measured by in situ FTIR (b). A decrease in absorbance and thus the disappearance of functional groups can be seen as dark blue regions, while an increase in absorbance and thus addition of functional groups is indicated in yellow.

modes.[57,58] The peak at 1230 cm^{-1} might be identified as the longitudinal optic component of the Si−O−Si stretch, but the peak might as well be a spurious feature caused by the subtraction of the Si reference sample that displays strong absorption peaks in this region.[59] All observed features are in agreement with the ATR-FTIR report of Vos et al.,[31] confirming the deposition of a N_3-SAM by silanization of 11-azidoundecyltrimethoxysilane on a Si surface with native SiO_2.

In situ reflection FTIR measurements are performed every 7 min on a N_3-SAM coated TiN substrate with a thin layer of SiO_2, to observe any changes of the functional groups over time in high vacuum at a pressure of 1×10^{-5} mbar and a temperature of 150 °C. The time evolution of the FTIR signal is shown in Figure 2 b. Light blue corresponds to zero changes in IR absorbance compared to the initial situation. Regions with a dark blue colour represent a decrease in IR absorbance and associated removal of functional groups, while yellow regions display an increase in absorbance and accordingly an addition of functional groups. Despite the fact that multiple lines become visible, only two features show a clear gradient trend over the full time in vacuum. One feature displays the increase in IR absorbance at around 1267 cm^{-1}. The identification of this peak is complex as several functional groups such as C−N, Si−O and C−H present features in this region.[56,57,59,60] Due to the shape of the curve - a sharp increase with neighbouring drop - a blue shift of the feature at 1230 cm^{-1} is suspected. As previously described, this feature might be identified as the longitudinal optical phonon mode of SiO_2 originating from the silane molecules chemisorbed at the surface and/or the SiO_2 substrate. It is known from literature that the longitudinal optical phonon mode Si−O−Si stretch shifts upon changes in Si−O bonding angle, bond length, force constant, image charge effects and total oxide thickness.[59,61–63]

Another prominent feature is the decrease in IR absorbance at 2105 cm^{-1}, related to the disappearance of the azido-group. This degradation of the azido-group is not expected in high vacuum and the temperature of 150 °C is well below the decomposition temperature

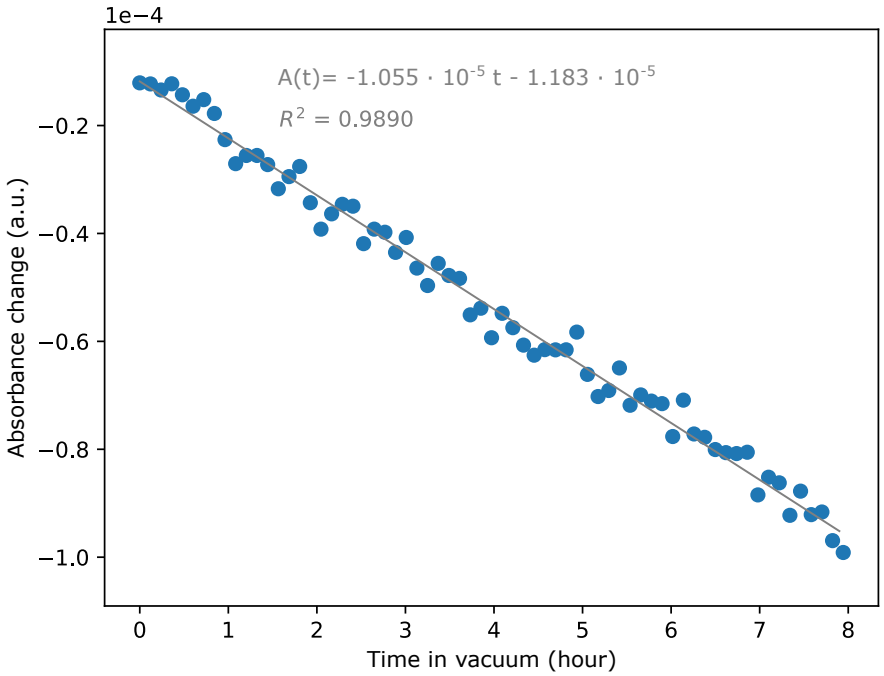

Figure 3: The evolution of the peak height of the antisymmetric azide stretching mode at $2105\,\mathrm{cm}^{-1}$ over time in high vacuum. The line indicates a linear fit to the data, the fit equation and goodness of fit are displayed next to the data.

of 180 °C reported for alkyl azides in literature.[41,43] The decrease in IR absorbance of the antisymmetric azide stretching mode in high vacuum over time is shown in Figure 3. The linear trend implies zero order reaction kinetics for the degradation of the azides during the 8 hour time interval of the observations. As will be discussed later, analysis of the ATR-FTIR data shows that 79 % of the azides are still remaining at the surface after 8 h in vacuum at 150 °C and a pressure of 1×10^{-5} mbar.

Not the complete silane molecule is desorbing from the surface, which can occur during the deposition of SAMs via vapour phase silanization before the formation of a stable monolayer by chemisorption to the surface.[64,65] After chemisorption to the surface, the silane molecules are reported to be stable under ultra high vacuum conditions up to 250 °C, depending on the end group and length of the carbon chain.[66,67] In the case that complete silane molecules would be disappearing from the surface, the decrease in the absorbance of the azide stretching mode should be accompanied by a decrease in the absorbance of the CH_2 stretches at 2925 cm^{-1} and 2855 cm^{-1}. However, after an initial drop in IR absorption intensity during the first half hour in vacuum, the CH_2 absorbance seems to remain constant. This is demonstrated more clearly in Figure S3 in the supporting information where the FTIR spectrum after approximately 36 min in vacuum is used as starting point to display the time evolution, and in Figure S4 presenting the evolution of the peak height of the CH_2 stretching vibrations over time. The initial decrease in IR absorbance is probably related to the removal of organic contamination from exposure of the surface to air. This is supported by the drop observed at 2960 cm^{-1}, which is most likely assigned to CH_3 stretches originating from organic contamination, decreasing with a similar rate as the CH_2 stretches after which it remains constant. The observations thus imply that the carbon chain of the silane molecules remains intact while the azido-group disappears. This is also indicated by contact angle measurements performed on the sample after vacuum treatment and on a N_3-SAM reference sample, which are respectively $(86.43 \pm 0.40)^\circ$ and $(83.1 \pm 1.3)^\circ$. Upon removal of complete silane molecules from the N_3-SAM by for example photocatalytic degradation on a TiO_2 surface, the contact

angle is observed to decrease with tens of degrees due to the removal of the hydrophobic carbon chain and exposure of hydrophilic hydroxyl groups at the surface.[68]

To our knowledge few literature reports mention the degradation of azides in high vacuum. Bebensee et al.[33] observed a low yield of the azide-alkyne click-reaction in ultra high vacuum on Cu(111). They concluded from XPS measurements that most azides decomposed and lost nitrogen upon sublimation on the metal surface. They suggest charge transfer from the metal surface might play a role in the degradation mechanism. Diaz et al.[32] investigated the azide-alkyne click-reaction in ultra high vacuum on Au(111) by the deposition of N-(4-azidophenyl)-4-ethynylbenzamide. Using scanning tunnelling microscopy they detected a disordered molecular phase indicating the degradation of the azide on the metal surface and confirming the findings of Bebensee et al. In the present work, N_3-SAM is found to degrade directly on top of a SiO_2 surface in high vacuum, excluding the charge transfer from a metal surface as a possible degradation mechanism. Gao et al.[45] exposed a ZnO surface to benzyl azide for 45 min at 100 °C in a high vacuum chamber with a pressure of 1×10^{-6} mbar. The benzyl azide was dosed into the chamber with a pressure of 1 mbar. XPS measurements displayed a low broad feature around 400 eV likely corresponding to surface bound nitrene species originating from azido groups directly reacting with ZnO after the loss of nitrogen as predicted by density functional theory calculations. The degradation of the azide was not further examined as the aim of their paper was to demonstrate the successful gas-phase copper catalysed and copper free azide-alkyne click reaction for surface functionalization of ZnO. Also other nitrogen-containing species such as carboxybetaine polymer brushes have been observed to decompose in the high vacuum conditions using XPS measurements. Both Van Andel et al.[69] and Kuzmyn et al.[70] report the disappearance of the ammonium peak in the N1s spectra of carboxybetaine polymer brushes upon prolonged waiting time inside the ultrahigh vacuum chamber of the XPS.

The most dominant degradation mechanism of alkyl azides reported in literature involves

the loss of nitrogen and the formation of a highly reactive nitrene intermediate species. This reaction mechanism is observed for the thermolysis of alkyl azides,[41–44] the degradation of azides upon X-ray exposure[36,37] and for the photolysis of alkyl azides upon irradiation with UV-light.[39–41] For the latter, other reaction mechanisms that bypass the nitrene intermediate and immediately rearrange into an imine are reported as well.[38,71] Nitrenes only have a very short lifetime and rapidly undergo stabilization via several reaction pathways including recombination into an azo compound (N=N), insertion into C-H bonds with formation of amines and the most common pathway isomerization into an imine (C=N).[41,43]

The C=N stretching band of an imine occurs in the region 1690 cm^{-1} to 1640 cm^{-1}.[56,57,72] Alkyl azo compounds present a weak N=N stretching band in the region 1580 cm^{-1} to 1530 cm^{-1}.[56,73,74] The in situ FTIR data and ATR-FTIR spectra after degradation show no clear addition of absorption features in these regions, implying that no imines or azo compounds are formed upon the removal of azides. However, it has to be emphasized that not all azides in the monolayer are degraded and the intensity of the IR absorption band due to the antisymmetric azide stretching vibration is strong compared to other functional groups. Therefore, the IR intensity of the imines and azo compounds might be too weak to be observed. For the same reason, the absence of the sharp characteristic N−H stretching vibration in the region 3450 cm^{-1} to 3250 cm^{-1} due to primary or secondary amines, can not exclude their existence.[57,60,75] Nedel'ko et al.[76] observed cross-linking of chains upon the thermal degradation of an azide containing oligomer and the formation of azo compounds, secondary amines and imines. Analogously, all before mentioned functional groups might be formed in this work upon degradation of the azido-group of the N_3-SAM and subsequent reaction with the neighbouring alkane chains. Saad et al.[37] even suggest the formation of tertiary amines for the X-ray induced degradation of azides through cleavage of the C−C bonds of adjacent alkane chains. The peak arising at 1267 cm^{-1} in the in situ FTIR data might be a manifestation of the C−N stretching vibration of these tertiary amines.[57,60] However, as described previously exact identification of the peak at 1267 cm^{-1} is complex.

The time evolution of the peak at 1267 cm^{-1} seems to follow first order reaction kinetics (Figure S5 in the supporting information) in contrast to the zero order reaction kinetics observed for the azide degradation, implying both features are not related to the same chemical reaction and the cumbersome identification of the peak at 1267 cm^{-1} will thus not change the conclusion that azido-groups degrade in high vacuum. XPS measurements are performed on degraded N_3-SAM samples since insufficient information can be extracted from the FTIR data to identify the most common degradation products. As can been seen in Figure S6 two peaks are observed at 404.4 - 404.5 eV and 400.8 eV in the N1s spectra, which can be assigned to the central and outer nitrogen atoms of the azido-group respectively.[31,77,78] The intensity of these peaks is observed to be lower for the degraded N_3-SAM samples. In addition, an extra feature is found to arise upon degradation of the azido-groups at 399.3 eV. This peak can be assigned to amine, imine and azo compounds, which are all possible degradation products of the azido-groups as described previously.[79–81] The most common degradation product can thus not unambiguously be identified. Nevertheless, the XPS data is consistent with the FTIR data presenting the degradation of the azido-group under high vacuum.

As the azido-group commonly degrades with the loss of a nitrogen molecule, the degradation reaction might be hindered by presence of nitrogen gas. In addition, the degradation reaction rate typically depends on the temperature. Therefore, the degradation of the N_3-SAM is investigated at seven different nitrogen pressures and at three different temperatures. The percentage of remaining azide groups at the surface after a 8 h vacuum treatment is calculated by integrating the ATR-FTIR peak area of the antisymmetric azide stretch and comparing it to a reference N_3-SAM and a blank Si sample. All N_3-SAM spectra and their corresponding references can be found in Figure S7 in the supporting information. The calculated percentage of azide remaining at the surface and corresponding contact angles for each sample can be seen in Figure S8. As expected, the resulting temperature-pressure graph in Figure 4 shows less degradation at lower temperatures and higher nitrogen pressures. The

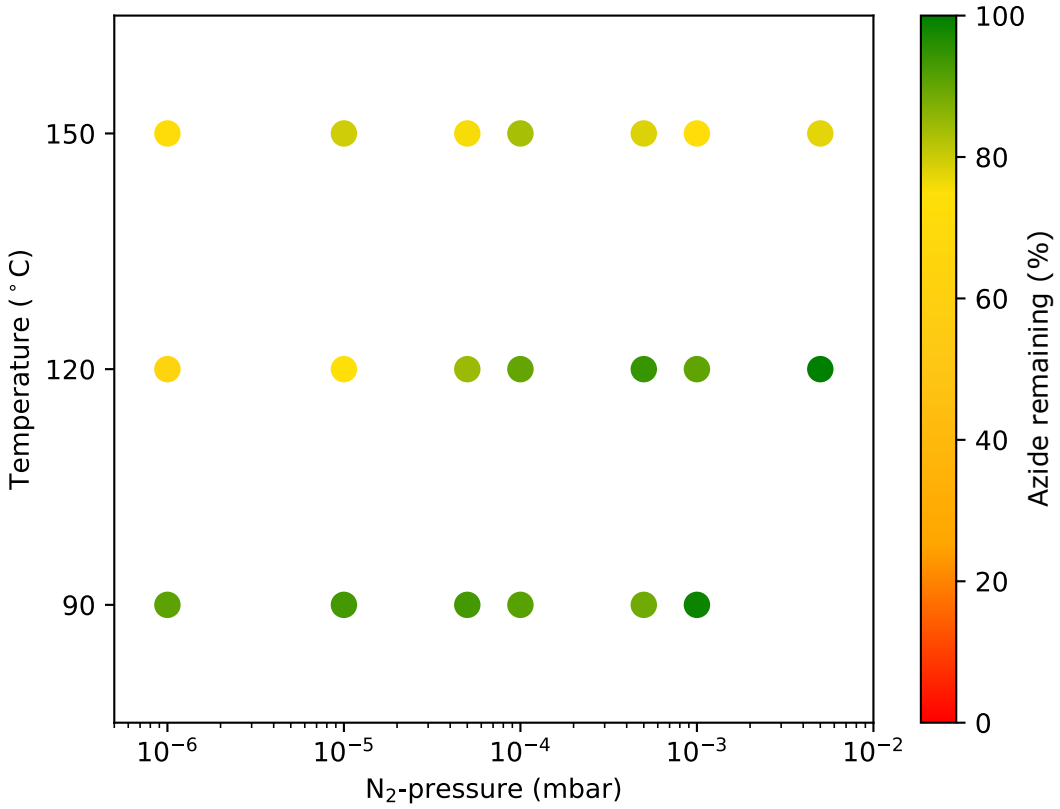

Figure 4: The percentage of azides remaining at the N_3-SAM surface after 8 h in vacuum for three different temperatures and seven different nitrogen pressures. The colours are an artistic impression meant to provide qualitative information. The reader is referred to Figure S9 in the supporting information for a quantitative visualisation of the data.

influence of the nitrogen pressure is in line with the proposed degradation mechanism for the azide, involving the loss of a nitrogen molecule and the formation of a highly reactive nitrene:

$$R{-}N_3 \rightleftharpoons R{-}N^{\cdot} + N_2$$

Unfortunately, in this work no equilibrium is obtained after 8 h in high vacuum. The improved stability at high nitrogen pressures explains why no azide degradation is observed by Vos et al.[31] when comparing a N_3-SAM deposited from the vapour phase in a vacuum chamber with a base pressure of 25 mbar to a N_3-SAM film prepared via the solvent phase. In addition, it clarifies why no degradation in vacuum is detected by Saric et al.,[34,35] when using azide and alkyne precursors as building blocks for MLD growth on top of ZnO and

ZrO_2 surfaces, since in that work nitrogen is used as delivery and purge gas at a pressure of 1 mbar and the substrate temperature ranges from 70 °C to 150 °C. For ALD/MLD growth using azide-based precursors the use of nitrogen purged type reactors instead of pump type reactors might thus be required to grow continuous pin-hole free coatings.

For the highest degradation detected, merely 63 % of the azides are remaining at the N_3-SAM surface after 8 h in vacuum. This is a significant loss in amount of azide groups introduced after functionalization. With miniaturization being the general trend in semiconductor industry, exact control of the surface functionalization down to the nanometre scale is of utmost importance to obtain reproducible results. For example regarding biosensor devices, the azide degradation not only means removal of functional groups at the surface for further click reactions, the degradation products might also introduce sites for the non-specific binding of biomolecules and thus increase the noise level of biosensor devices.[82] In addition, the density of functional groups at the surface for immobilization of biomolecules might influence the orientation of the molecules and have a significant effect on the signal obtained during biological assays.[83] Various applications require patterned micro- and nanostructures using azide based chemistry.[68] Therefore, one should be aware of the azide degradation altering the foreseen surface functionalization, not only during deposition of an azido-containing film in high vacuum but also when performing processing steps in vacuum after the introduction of azido-groups to the surface.

4 Conclusion

The degradation of the azido-groups of a N_3-SAM is observed under high vacuum conditions using in situ FTIR. The rate of degradation is found to dependent on the time, sample temperature and the nitrogen pressure introduced into the vacuum system. Many applications in the semiconductor industry require exact control of the surface functionalization down to the nanometre level to achieve reproducible results. The degradation of the azido groups

in high vacuum inevitably leads to a loss in control of the exact surface functionalization. Therefore, the azide stability should always be evaluated when depositing or post-processing azido-containing coatings in high vacuum.

Supporting Information

Data-analysis of the in situ FTIR data with Python; Ex situ transmission FTIR spectra of the as-deposited N_3-SAM sample and the Si reference; In situ FTIR data plotted with starting point at 36 min; Evolution of the absorbance change over time in high vacuum of the CH_2 stretching vibrations as measured by in situ FTIR; Evolution of the absorbance change over time in high vacuum of the feature at 1267 cm^{-1} as measured by in situ FTIR; N1s XPS spectra of a N_3-SAM reference and two degraded samples; All ATR-FTIR spectra, the resulting percentages of azide remaining on the surface and the contact angle of each sample; Quantitative visualisation of the percentage of azides remaining at the N_3-SAM surface for different temperatures and nitrogen pressures.

Acknowledgements

The authors acknowledge BOF-UGent (GOA-01G01019) for financial support. Nisula M. thanks the Marie Skłodowska-Curie Actions (grant agreement no. 841995) for a postdoctoral fellowship. We thank Leliaert J. and Dobbels W. for helpful discussions on the FTIR background subtraction via Python. We thank Li J. to perform the XPS measurements.

References

(1) Kolb, H. C.; Finn, M.; Sharpless, K. B. Click chemistry: diverse chemical function from a few good reactions. *Angew. Chem., Int. Ed.* **2001**, *40*, 2004–2021.

(2) Lahann, J. *Click chemistry for biotechnology and materials science*; John Wiley & Sons, Ltd: Chichester, UK, 2009; Chapter 1, pp 1–7.

(3) Chen, Y. In *Click chemistry: Approaches, applications and challenges*; Chen, Y., Tong, Z.-R., Eds.; Nova Science Publishers: New York, 2017; Chapter 1, pp 1–19.

(4) Moses, J. E.; Moorhouse, A. D. The growing applications of click chemistry. *Chem. Soc. Rev.* **2007**, *36*, 1249–1262.

(5) Jiang, X.; Hao, X.; Jing, L.; Wu, G.; Kang, D.; Liu, X.; Zhan, P. Recent applications of click chemistry in drug discovery. *Expert Opin. Drug Discovery* **2019**, *14*, 779–789.

(6) Kolb, H. C.; Sharpless, K. B. The growing impact of click chemistry on drug discovery. *Drug discovery today* **2003**, *8*, 1128–1137.

(7) Golas, P. L.; Matyjaszewski, K. Marrying click chemistry with polymerization: expanding the scope of polymeric materials. *Chem. Soc. Rev.* **2010**, *39*, 1338–1354.

(8) Binder, W. H.; Sachsenhofer, R. 'Click' chemistry in polymer and materials science. *Macromol. Rapid Commun.* **2007**, *28*, 15–54.

(9) Xi, W.; Scott, T. F.; Kloxin, C. J.; Bowman, C. N. Click chemistry in materials science. *Adv. Funct. Mater.* **2014**, *24*, 2572–2590.

(10) Nandivada, H.; Jiang, X.; Lahann, J. Click chemistry: versatility and control in the hands of materials scientists. *Adv. Mater.* **2007**, *19*, 2197–2208.

(11) Gong, Y.; Pan, L. Recent advances in bioorthogonal reactions for site-specific protein labeling and engineering. *Tetrahedron Lett.* **2015**, *56*, 2123–2132.

(12) Pickens, C. J.; Johnson, S. N.; Pressnall, M. M.; Leon, M. A.; Berkland, C. J. Practical considerations, challenges, and limitations of bioconjugation via azide–alkyne cycloaddition. *Bioconjugate Chem.* **2017**, *29*, 686–701.

(13) McKay, C. S.; Finn, M. Click chemistry in complex mixtures: bioorthogonal bioconjugation. *Chem. Biol.* **2014**, *21*, 1075–1101.

(14) Rusmini, F.; Zhong, Z.; Feijen, J. Protein immobilization strategies for protein biochips. *Biomacromolecules* **2007**, *8*, 1775–1789.

(15) Trilling, A. K.; Beekwilder, J.; Zuilhof, H. Antibody orientation on biosensor surfaces: a minireview. *Analyst* **2013**, *138*, 1619–1627.

(16) Dietrich, P. M.; Lange, N.; Lippitz, A.; Holzweber, M.; Kulak, N.; Unger, W. Click chemistry on silicon nitride for biosensor fabrication. *Appl. Surf. Sci.* **2019**, *481*, 10–15.

(17) Hong, T.; Liu, W.; Li, M.; Chen, C. Click chemistry at the microscale. *Analyst* **2019**, *144*, 1492–1512.

(18) Bock, V. D.; Hiemstra, H.; Van Maarseveen, J. H. CuI-catalyzed alkyne–azide "click" cycloadditions from a mechanistic and synthetic perspective. *Eur. J. Org. Chem.* **2006**, *2006*, 51–68.

(19) Dommerholt, J.; Rutjes, F. P.; van Delft, F. L. In *Cycloadditions in bioorthogonal chemistry*; Vrabel, M., Carell, T., Eds.; Springer, Cham.: Zwitserland, 2016; pp 57–76.

(20) Manova, R.; van Beek, T. A.; Zuilhof, H. Surface functionalization by strain-promoted alkyne–azide click reactions. *Angew. Chem., Int. Ed.* **2011**, *50*, 5428–5430.

(21) Haensch, C.; Hoeppener, S.; Schubert, U. S. Chemical modification of self-assembled silane based monolayers by surface reactions. *Chem. Soc. Rev.* **2010**, *39*, 2323–2334.

(22) Debrassi, A.; Roeven, E.; Thijssen, S.; Scheres, L.; de Vos, W. M.; Wennekes, T.; Zuilhof, H. Versatile (bio) functionalization of bromo-terminated phosphonate-modified porous aluminum oxide. *Langmuir* **2015**, *31*, 5633–5644.

(23) Al-Hajj, N.; Mousli, Y.; Miche, A.; Humblot, V.; Hunel, J.; Heuze, K.; Buffeteau, T.; Genin, E.; Vellutini, L. Influence of the grafting process on the orientation and the reactivity of azide-terminated monolayers onto silica surface. *Appl. Surf. Sci.* **2020**, *527*, 146778.

(24) Pujari, S. P.; Scheres, L.; Marcelis, A. T.; Zuilhof, H. Covalent surface modification of oxide surfaces. *Angew. Chem., Int. Ed.* **2014**, *53*, 6322–6356.

(25) Onclin, S.; Ravoo, B. J.; Reinhoudt, D. N. Engineering silicon oxide surfaces using self-assembled monolayers. *Angew. Chem., Int. Ed.* **2005**, *44*, 6282–6304.

(26) Ulman, A. Formation and structure of self-assembled monolayers. *Chem. Rev.* **1996**, *96*, 1533–1554.

(27) Liang, L.; Astruc, D. The copper (I)-catalyzed alkyne-azide cycloaddition (CuAAC) "click" reaction and its applications. An overview. *Coord. Chem. Rev.* **2011**, *255*, 2933–2945.

(28) Williams, M. G.; Teplyakov, A. V. Building high-coverage monolayers of covalently bound magnetic nanoparticles. *Appl. Surf. Sci.* **2016**, *388*, 461–467.

(29) Rostovtsev, V. V.; Green, L. G.; Fokin, V. V.; Sharpless, K. B. A stepwise huisgen cycloaddition process: copper (I)-catalyzed regioselective "ligation" of azides and terminal alkynes. *Angew. Chem.* **2002**, *114*, 2708–2711.

(30) Lowe, R. D. Controlled vapor deposition of azide-terminated siloxane monolayers: a platform for tailoring oxide surfaces. Ph.D. thesis, Stanford University Stanford, CA, 2011.

(31) Vos, R.; Rolin, C.; Rip, J.; Conard, T.; Steylaerts, T.; Cabanilles, M. V.; Levrie, K.; Jans, K.; Stakenborg, T. Chemical vapor deposition of azidoalkylsilane monolayer films. *Langmuir* **2018**, *34*, 1400–1409.

(32) Díaz Arado, O.; Mönig, H.; Wagner, H.; Franke, J.-H.; Langewisch, G.; Held, P. A.; Studer, A.; Fuchs, H. On-surface azide–alkyne cycloaddition on Au (111). *ACS nano* **2013**, *7*, 8509–8515.

(33) Bebensee, F.; Bombis, C.; Vadapoo, S.-R.; Cramer, J. R.; Besenbacher, F.; Gothelf, K. V.; Linderoth, T. R. On-surface azide–alkyne cycloaddition on Cu (111): does it "click" in ultrahigh vacuum? *J. Am. Chem. Soc.* **2013**, *135*, 2136–2139.

(34) Saric, I.; Peter, R.; Markovic, M. K.; Badovinac, I. J.; Rogero, C.; Ilyn, M.; Knez, M.; Ambrožić, G. Introducing the concept of pulsed vapor phase copper-free surface click-chemistry using the ALD technique. *Chem. Commun.* **2019**, *55*, 3109–3112.

(35) Šarić, I.; Markovic, M. K.; Peter, R.; Linić, P.; Wittine, K.; Piltaver, I. K.; Badovinac, I. J.; Marković, D.; Knez, M.; Ambrožić, G. In-situ multi-step pulsed vapor phase surface functionalization of zirconia nanoparticles via copper-free click chemistry. *Appl. Surf. Sci.* **2021**, *539*, 148254.

(36) Schulze, R.; Boyd, D.; Evans, J. F.; Gladfelter, W. L. A variable temperature x-ray photoelectron spectroscopic study of the surface conversion of diethylaluminum azide to AlN. *J. Vac. Sci. Technol., A* **1990**, *8*, 2338–2343.

(37) Saad, A.; Abderrabba, M.; Chehimi, M. M. X-ray induced degradation of surface bound azido groups during XPS analysis. *Surf. Interface Anal.* **2017**, *49*, 340–344.

(38) Abramovitch, R. A.; Kyba, E. Photodecomposition of alkyl azides. Absence of freedom of choice and nonnitrene mechanism. *J. Am. Chem. Soc.* **1971**, *93*, 1537–1538.

(39) Klima, R. F.; Gudmundsdóttir, A. D. Intermolecular triplet-sensitized photolysis of alkyl azides: Trapping of triplet alkyl nitrenes. *J. Photochem. Photobiol., A* **2004**, *162*, 239–247.

(40) Currie, C.; Darwent, B. d. The photochemical decomposition of methyl azide. *Can. J. Chem.* **1963**, *41*, 1552–1559.

(41) Abramovitch, R. A.; Banthorpe, D. V.; Biffin, M. E. C.; Gurst, J. E.; Kyba, E. P.; Lwowski, W.; Miller, J.; Paul, D. B.; Pryde, C. A.; Reiser, A.; Sheradsky, T.; Smolinsky, G.; Treinin, A.; Wagner, H. M. In *Chemistry of the azido group*; Patai, S., Ed.; Interscience Publishers: New York, 1971; pp 21–23, 245, 442 –444, 461–486.

(42) Abramovitch, R.; Kyba, E. Thermolysis of tertiary alkyl azides. *J. Am. Chem. Soc.* **1974**, *96*, 480–488.

(43) L'abbe, G. Decomposition and addition reactions of organic azides. *Chem. Rev.* **1969**, *69*, 345–363.

(44) Kyba, E. P. In *Azides and nitrenes, reactivity and utility*; Scriven, E. F. V., Ed.; Academic Press Inc.: Orlando, Florida, 1984; Chapter 1, pp 2–34.

(45) Gao, F.; Aminane, S.; Bai, S.; Teplyakov, A. V. Chemical protection of material morphology: robust and gentle gas-phase surface functionalization of ZnO with propiolic acid. *Chem. Mater.* **2017**, *29*, 4063–4071.

(46) Aswal, D.; Lenfant, S.; Guerin, D.; Yakhmi, J.; Vuillaume, D. Self assembled monolayers on silicon for molecular electronics. *Anal. Chim. Acta* **2006**, *568*, 84–108.

(47) Duwez, A.-S. Exploiting electron spectroscopies to probe the structure and organization of self-assembled monolayers: a review. *J. Electron Spectrosc. Relat. Phenom.* **2004**, *134*, 97–138.

(48) Vandenbroucke, S. S.; Levrau, E.; Minjauw, M. M.; Van Daele, M.; Solano, E.; Vos, R.; Dendooven, J.; Detavernier, C. Study of the surface species during thermal and plasma-enhanced atomic layer deposition of titanium oxide films using in situ IR-spectroscopy

and in vacuo X-ray photoelectron spectroscopy. *Phys. Chem. Chem. Phys.* **2020**, *22*, 9262–9271.

(49) Fringeli, U. In *Encyclopedia of spectroscopy and spectrometry*; Lindon, J. C., Ed.; Elsevier: Oxford, 1999; pp 58–64.

(50) Rabolt, J.; Jurich, M.; Swalen, J. Infrared reflection-absorption studies of thin films at grazing incidence. *Appl. Spectrosc.* **1985**, *39*, 269–272.

(51) Greenler, R. G. Infrared study of adsorbed molecules on metal surfaces by reflection techniques. *J. Chem. Phys.* **1966**, *44*, 310–315.

(52) Van Rossum, G.; Drake, F. L. *Python 3 reference manual*; CreateSpace: Scotts Valley, CA, 2009.

(53) Sondag, A.; Raas, M.; Van Velzen, P. Contamination of aluminium oxide surfaces in ambient air investigated by FTIR MSR and TOF SIMS. Chemisorption of aliphatic carboxylic acids. *Chem. Phys. Lett.* **1989**, *155*, 503–510.

(54) Vairavamurthy, A.; Roberts, J. M.; Newman, L. Methods for determination of low molecular weight carbonyl compounds in the atmosphere: a review. *Atmos. Environ., Part A* **1992**, *26*, 1965–1993.

(55) Snyder, R.; Strauss, H.; Elliger, C. Carbon-hydrogen stretching modes and the structure of n-alkyl chains. 1. Long, disordered chains. *J. Phys. Chem.* **1982**, *86*, 5145–5150.

(56) Lin-Vien, D.; Colthup, N. B.; Fateley, W. G.; Grasselli, J. G. *The handbook of infrared and Raman characteristic frequencies of organic molecules*; Academic Press: San Diego, 1991; pp 9–19, 197, 200–202, 221.

(57) Socrates, G. *Infrared and Raman characteristic group frequencies: tables and charts*, 3rd ed.; John Wiley & Sons: Chichester, 2001; pp 50–53, 78, 90, 107–112.

(58) Lieber, E.; Rao, C. N. R.; Chao, T. S.; Hoffman, C. W. W. Infrared spectra of organic azides. *Anal. Chem.* **1957**, *29*, 916–918.

(59) Tian, R.; Seitz, O.; Li, M.; Hu, W.; Chabal, Y. J.; Gao, J. Infrared characterization of interfacial Si- O bond formation on silanized flat SiO_2/Si surfaces. *Langmuir* **2010**, *26*, 4563–4566.

(60) Smith, B. C. *Infrared spectral interpretation: a systematic approach*; CRC press: Boca Raton, Florida, 2018; pp 135–141.

(61) Nagai, N.; Hashimoto, H. FT-IR-ATR study of depth profile of SiO_2 ultra-thin films. *Appl. Surf. Sci.* **2001**, *172*, 307–311.

(62) Giustino, F.; Pasquarello, A. Infrared spectra at surfaces and interfaces from first principles: Evolution of the spectra across the Si (100)-SiO_2 interface. *Phys. Rev. Lett.* **2005**, *95*, 187402.

(63) Queeney, K.; Weldon, M.; Chang, J.; Chabal, Y.; Gurevich, A.; Sapjeta, J.; Opila, R. Infrared spectroscopic analysis of the Si/SiO_2 interface structure of thermally oxidized silicon. *J. Appl. Phys.* **2000**, *87*, 1322–1330.

(64) Markov, A.; Greben, K.; Mayer, D.; Offenhaausser, A.; Wordenweber, R. In situ analysis of the growth and dielectric properties of organic self-assembled monolayers: A way to tailor organic layers for electronic applications. *ACS Appl. Mater. Interfaces* **2016**, *8*, 16451–16456.

(65) Yuan, X.; Wolf, N.; Mayer, D.; Offenhausser, A.; Wordenweber, R. Vapor-phase peposition and electronic characterization of 3-aminopropyltriethoxysilane self-assembled monolayers on silicon dioxide. *Langmuir* **2019**, *35*, 8183–8190.

(66) Chandekar, A.; Sengupta, S. K.; Whitten, J. E. Thermal stability of thiol and silane monolayers: A comparative study. *Appl. Surf. Sci.* **2010**, *256*, 2742–2749.

(67) Bhairamadgi, N. S.; Pujari, S. P.; Trovela, F. G.; Debrassi, A.; Khamis, A. A.; Alonso, J. M.; Al Zahrani, A. A.; Wennekes, T.; Al-Turaif, H. A.; van Rijn, C., et al. Hydrolytic and thermal stability of organic monolayers on various inorganic substrates. *Langmuir* **2014**, *30*, 5829–5839.

(68) Vandenbroucke, S. S. T.; Mattelaer, F.; Jans, K.; Detavernier, C.; Stakenborg, T.; Vos, R. Photocatalytic lithography with atomic layer-deposited TiO_2 films to tailor biointerface properties. *Adv. Mater. Interfaces* **2019**, *6*, 1900035.

(69) van Andel, E.; Lange, S. C.; Pujari, S. P.; Tijhaar, E. J.; Smulders, M. M.; Savelkoul, H. F.; Zuilhof, H. Systematic comparison of zwitterionic and non-zwitterionic antifouling polymer brushes on a bead-based platform. *Langmuir* **2018**, *35*, 1181–1191.

(70) Kuzmyn, A. R.; Nguyen, A. T.; Teunissen, L. W.; Zuilhof, H.; Baggerman, J. Antifouling polymer brushes via oxygen-tolerant surface-initiated PET-RAFT. *Langmuir* **2020**, *36*, 4439–4446.

(71) Kyba, E. P.; Abramovitch, R. A. Photolysis of alkyl azides. Evidence for a nonnitrene mechanism. *J. Am. Chem. Soc.* **1980**, *102*, 735–740.

(72) Stolkin, I.; Ha, T.-K.; Günthard, H. H. N-methylmethyleneimine and ethylideneimine: gas-and matrix-infrared spectra, ab initio calculations and thermodynamic properties. *J. Chem. Phys.* **1977**, *21*, 327–347.

(73) Le Fevre, J.; O'Dwyer, M.; Werner, R. Infra-red spectra of compounds containing the azo-group. *Aust. J. Chem.* **1953**, *6*, 341–359.

(74) Durig, J.; Pate, C.; Harris, W. Vibrational spectra and structure of azomethane and azomethane-d 6. *J. Chem. Phys.* **1972**, *56*, 5652–5662.

(75) Alpert, N. L.; Keiser, W. E.; Szymanski, H. A. *IR: theory and practice of infrared spectroscopy*; Springer Science & Business Media: Boston, MA, 2012; pp 277–281.

(76) Nedel'ko, V.; Korsunskii, B.; Shastin, A.; Larikova, T.; Badamshina, E.; Lodygina, V.; Ol'khova, O.; Zaverkina, M. Thermal degradation of bis (azidomethyl) oxethane oligomer. *Polym. Sci., Ser. B* **2007**, *49*, 1–5.

(77) Gouget-Laemmel, A.; Yang, J.; Lodhi, M.; Siriwardena, A.; Aureau, D.; Boukherroub, R.; Chazalviel, J.-N.; Ozanam, F.; Szunerits, S. Functionalization of azide-terminated silicon surfaces with glycans using click chemistry: XPS and FTIR study. *J. Phys. Chem. C* **2013**, *117*, 368–375.

(78) Darlatt, E.; Traulsen, C. H.-H.; Poppenberg, J.; Richter, S.; Kühn, J.; Schalley, C. A.; Unger, W. E. Evidence of click and coordination reactions on a self-assembled monolayer by synchrotron radiation based XPS and NEXAFS. *J. Electron Spectrosc. Relat. Phenom.* **2012**, *185*, 85–89.

(79) Kehrer, M.; Duchoslav, J.; Hinterreiter, A.; Cobet, M.; Mehic, A.; Stehrer, T.; Stifter, D. XPS investigation on the reactivity of surface imine groups with TFAA. *Plasma Processes and Polym.* **2019**, *16*, 1800160.

(80) Shircliff, R. A.; Stradins, P.; Moutinho, H.; Fennell, J.; Ghirardi, M. L.; Cowley, S. W.; Branz, H. M.; Martin, I. T. Angle-resolved XPS analysis and characterization of monolayer and multilayer silane films for DNA coupling to silica. *Langmuir* **2013**, *29*, 4057–4067.

(81) Pang, W.; Xue, J.; Pang, H. A high energy density azobenzene/graphene oxide hybrid with weak nonbonding interactions for solar thermal storage. *Sci. rep.* **2019**, *9*, 1–12.

(82) Hassibi, A.; Vikalo, H.; Hajimiri, A. On noise processes and limits of performance in biosensors. *J. Appl. Phys.* **2007**, *102*, 014909.

(83) White, R. J.; Phares, N.; Lubin, A. A.; Xiao, Y.; Plaxco, K. W. Optimization of electrochemical aptamer-based sensors via optimization of probe packing density and surface chemistry. *Langmuir* **2008**, *24*, 10513–10518.

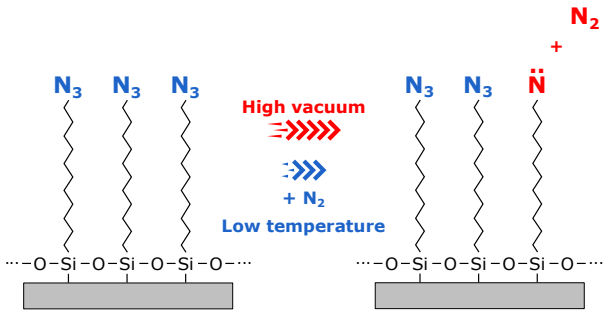

For Table of Contents Only.